Water Research 216 (2022) 118348

Contents lists available at ScienceDirect

Water Research

journal homepage: www.elsevier.com/locate/watres

Prolonged heavy rainfall and land use drive catchment sediment source dynamics: Appraisal using multiple biotracers

Hari Ram Upadhayay [a,*], Yusheng Zhang [a], Steven J. Granger [a], Mafalda Micale [a,b], Adrian L. Collins [a]

[a] Sustainable Agriculture Sciences, Rothamsted Research, North Wyke, Okehampton, EX20 2SB, United Kingdom
[b] Department of Agriculture, Università degli Studi Mediterranea di Reggio Calabria, Reggio Calabria, Feo di Vito 89122, Italy

ARTICLE INFO

Keywords:
Extreme rainfall
Bound-fatty acids
Compound-specific stable isotopes
Bayesian mixing model
Sediment source fingerprinting

ABSTRACT

Excessive sediment loss degrades freshwater quality and is prone to further elevation and variable source contributions due to the combined effect of extreme rainfall and differing land uses. To quantify erosion and sediment source responses across scales, this study integrated work at both field and catchment scale for two hydrologically contrasting winters (2018–19 and 2019–20). Sediment load was estimated at the field scale (grassland-arable conversion system). Sediment source apportionment work was undertaken at the catchment scale (4.5 km^2) and used alkanes, and both free and bound fatty acid carbon isotope signatures as diagnostic fingerprints to distinguish sediment sources: arable, pasture, woodland and stream banks. Sediment source apportionment based on bound fatty acids revealed a substantial shift in contributions, from stream banks dominating (70 ± 5%) in winter 2018–19, to arable land dominating (52 ± 7%) in the extreme wet winter 2019–20. Increases in sediment contributions from arable (~3.9 times) and pasture (~2.4 times) land at the catchment outlet during the winter 2019–20 were consistent with elevated sediment losses monitored at the field scale which indicated that low-magnitude high frequency rainfall alone increased sediment loss even from pasture by 350%. In contrast, carbon isotope signatures of alkanes and free fatty acids consistently estimated stream banks as a dominant source (i.e., ~36% and ~70% respectively) for both winters regardless of prolonged rainfall in winter 2019–20. Beyond quantifying the shifts in field scale sediment load and catchment scale sediment sources due to the changes in rainfall patterns, our results demonstrate valuable insight into how the fate of biotracers in soil and sediment manifests in the $\delta^{13}C$ values of homologues and, in turn, their role in information gain for estimating sediment source contributions. Discrepancies in the estimated sediment source contributions using different biotracers indicate that without a careful appreciation of their biogeochemical limitations, erroneous interpretation of sediment source contributions can undermine management strategies for delivering more sustainable and resilient agriculture.

1. Introduction

Considerable research and policy interest continue to focus on mitigating agricultural water pollution including that associated with excessive fine-grained (<63 μm) sediment (Collins et al., 2020). Soil erosion by water incurs a huge burden for global GDP (Sartori et al., 2019) and water erosion is expected to increase 30–66% in the near future due to climate change (Borrelli et al., 2020). Excess sediment resulting from accelerated soil erosion by water can result in profound ecological impairment in aquatic ecosystems. The nutrients and contaminants released from deposited fine sediment into the water column are a common reason why 'good ecological status' (GES) is often not achieved in many waterbodies (Tye et al., 2016) despite the implementation of best management practices (BMPs).

Climate change is directly altering the trend and pattern of rainfall extremes leading to increased runoff which intensifies sediment generation processes (e.g., soil detachment and sediment delivery) in catchments (Li and Fang 2016). Thus, extreme and/or prolonged periods of heavy rainfall, have been identified as a major driver of water quality impairment. Equally, land use change/management is also widely seen as a key driver for changing sediment source dynamics in river systems globally. The effect of both heavy rainfall and land use change can have

* Corresponding author.
E-mail address: Hari.upadhayay@Rothamsted.ac.uk (H.R. Upadhayay).

https://doi.org/10.1016/j.watres.2022.118348
Received 6 December 2021; Received in revised form 14 March 2022; Accepted 21 March 2022
Available online 22 March 2022

synergistic or antagonistic effects on soil erosion and sediment delivery. However, there remains a significant knowledge gap concerning the relative role of these critical factors in driving sediment source dynamics at the catchment scale. Disentangling these roles is very important for helping to optimise BMPs.

Sediment source fingerprinting is one method that helps elucidate catchment sediment source and export dynamics in the context of key land use change and climatic drivers (see Collins et al., 2020 and references therein). In recent times, the use of vegetation-based biomarkers (hereafter biotracers), especially long-chain alkane and fatty acid specific stable isotopes has gained momentum within the sediment fingerprinting community due to their potential to help discriminate different land uses and sediment sources (Upadhayay et al., 2017). A key characteristic of biotracers is that their stable isotope signature varies across vegetation due to differences in plant physiology and environmental factors (Reiffarth et al., 2016). Long-chain alkanes and fatty acids (FAs) are biosynthesised by plants and transferred to soil where they are considered to be relatively resistant to degradation largely because of their lower aqueous solubility and microbial inaccessibility. Alkanes do not contain a reactive functional group and as they are chemically inert, they remain in soil aggregates as a part of soil organic matter. In contrast, FAs are pervasive (due to higher solubility than alkanes) in soil and are firmly attached to soil particles due to the -COOH functional group, moving with sediment in association with minerals and/or in an encapsulated form in water-stable aggregates. Studies on sediment source apportionment have so far mainly focused on solvent extractable (free) alkanes and/or fatty acids (FFA) concentrations and/or their carbon isotope values – reflecting mainly a plant leaf wax origin. Solvent extractable alkanes and FAs do not include ester-bound lipids and their carbon isotope values can be strongly indicative of recent land use and the associated vegetation they derive from (Bull et al., 2000). However, the use of biotracers in mixing models is not straight forward due to differences in biotracer attachment to soil and sediment and their degree of susceptibility to degradation during sediment transport and/or after deposition, which ultimately alters the original isotopic signature derived from contributing sources. Therefore, a more systematic study of the use of different biotracers in isolation, or in combination, is needed.

Ester-bound lipids (lipids release upon base hydrolysis after first removing solvent-extractable compounds) represent tightly incorporated lipids in soil microaggregates and mineral-organic matrices mainly derived from plant biopolymers - cutin and suberin. These biotracers are more resistant to microbial degradation and may survive better during long distance or temporal duration fluvial transport than solvent extractable lipids (Feng et al., 2015). Therefore, ester-bound fatty acids (also known as bound FAs; BFAs) may be more diagnostic of land use contributions to sediment than FFAs (Nierop et al., 2006) due to their more pronounced stability (Feng et al., 2010). Yet, the application of BFA-specific isotopes has received little attention in the context of sediment source apportionment using fingerprinting procedures, despite the ongoing need to explore and test different fingerprint properties, including biotracers, in different geoclimatic contexts (Collins et al., 2020; Diefendorf and Freimuth 2017; Jansen and Wiesenberg 2017). To date, BFAs and their isotopic compositions have been analysed predominantly in marine and lake sediments, and not in fluvial samples.

Elucidating the impact of land use and extreme wet weather on sediment source dynamics requires catchment scale work across multiple years. To date, and often driven by the logistical requirements and costs, many sediment source apportionment studies have focused on a single season or year thereby not necessarily providing an opportunity to disentangle land use and hydroclimatic drivers. Given this research gap, we investigated how hydroclimatic patterns and land use affected sediment source dynamics in a mixed-land use agricultural catchment in south west England. The specific objectives were: 1) to assess the applicability of different biotracer (alkanes, FFAs, BFAs) carbon isotope signatures for quantifying sediment source contributions at catchment scale, and; 2) to quantify the relative role of extreme winter rainfall and land use on sediment source dynamics. To achieve these objectives, biotracer carbon isotope values were used to apportion the potential sources (arable, pasture, woodland and stream banks) of suspended sediment collected during the winter months (October to March) of both 2018–2019 (winter 2018–19) and 2019–2020 (winter 2019–20). These consecutive years provided ample opportunity to meet our objectives since the total rainfall during winter 2018–19 was 9% lower than the long-term (1981–2010) winter period average (i.e., ~663 mm), whereas it was 18% higher during winter 2019–20. Indeed, the month of February 2020 was the fifth wettest month recorded in the UK since 1862 and experienced 237% of the long-term (1981–2010) average February rainfall (Tandon and Schultz 2020). The study duration therefore encapsulated a relatively 'dry' and a relatively 'wet' winter period.

2. Materials and methods

2.1. Study catchment characteristics

This research was conducted in the Cocktree sub-catchment (4.5 km^2) of the upper River Taw in south west England (Fig. 1a). The soil is classified as Gleysol and Cambisol with clay and silty-clay loam dominated soil textures and moderately acidic soil pH. The catchment surface has a predominantly northern aspect with a maximum slope of 15.5° Permeability is moderately slow due to a subsurface clay layer and, as a result, saturation-excess overland flow is very common in the catchment during winter which is often seasonally waterlogged. Long-term (1981–2010) mean annual rainfall is ~1053 mm (North Wyke) with 63% occurring during the study defined winter period.

Land use is dominated by grassland (62%) on slopes ranging between 0.1–15.5° which comprise periodically ploughed and reseeded (a mixture of rye grass and clover) and permanent pasture. Silage cuts occur 2 to 3 times per year during the summer months and chemical fertilizer and manures/slurry are typically spread to stimulate grass growth. The grassland is used for low-density grazing (cattle and sheep), which stops during the winter when livestock are housed to avoid poaching when soils are waterlogged. Arable farming (23%) with slopes ranging between 0.2–12.6° consists of rotations dominated by winter cereals (barley and wheat), and maize. Ploughing for arable crops extends up to a depth of 30 cm, and inorganic N:P:K fertilizers, as well as manure/slurry, are applied at recommended rates based on routine soil analyses and agronomic advice. Semi-natural woodland covers 15% of the catchment area on slopes ranging between 0.4–13.8° and is mainly located in the riparian zone (Fig. 1a).

2.2. Suspended sediment and catchment source sampling

Suspended sediment samples were collected during winter 2018–19 and winter 2019–20 at the catchment outlet using Phillips tubes (Phillips et al., 2000). Generally, sediment samples were retrieved every two months, but sediment was collected earlier when significant intervention was required to maintain the sediment traps. Visible large organic detritus was removed manually, and sediment was settled in a dark cool room for 7–10 days. Excess water was siphoned off without disturbing the settled sediment. The sediment samples were freeze dried. In total there were eight sediment samples for winter 2018–19 and nine samples for winter 2019–20. Equal masses of the sediment samples were combined to measure the particle size of sediment from the contrasting winters. The absolute particle size distribution was measured using a LISST-100x after removing organic matter using H_2O_2 followed by dispersal of the particles in an ultrasonic water bath for 5 min. Approximately 90% of the sediment samples were finer than 63 μm (Fig. S1). Since the study catchment is ungauged, it lacks flow and suspended sediment concentration data which hindered the estimation of sediment loads at the catchment scale.

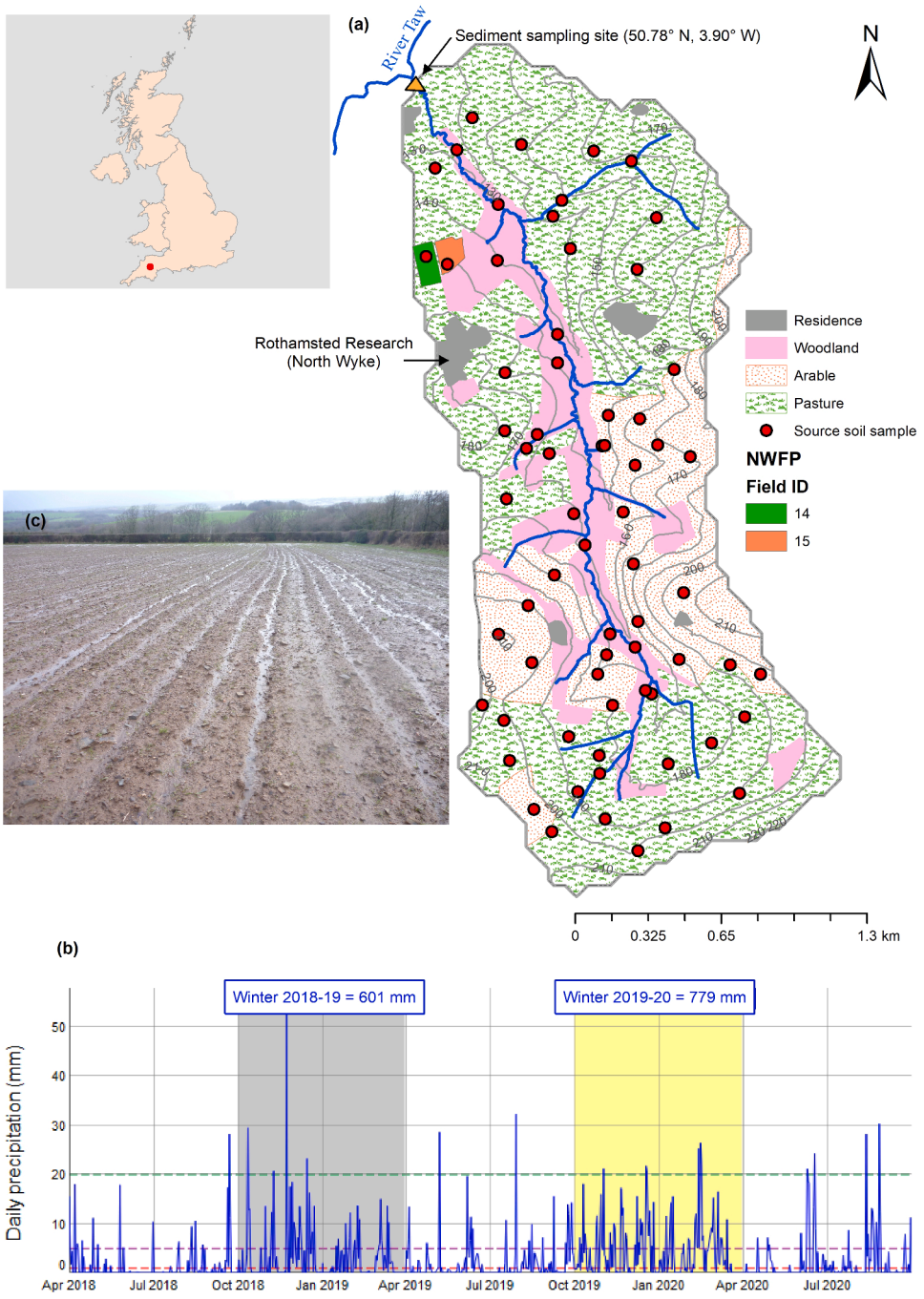

Fig. 1. Map of the Cocktree catchment showing: (a) the stream, land use and source and sediment sampling sites as well as the North Wyke Farm Platform (fields 14 and 15) and location in the UK; (b) the distribution of daily rainfall (red, purple and green horizontal dotted lines represent 1, 5 and 20 mm, respectively) during the study period and the total rainfall volumes for each winter period, and (c) a winter wheat field experiencing surface runoff during the early stages of crop development.

Four potential catchment sediment sources, namely arable (A), pasture (P), woodland (W) and stream banks (SB), were selected *a priori* based on a reconnaissance walkover. Composite surface (0 to 5 cm) soil samples (comprising a mixture of ~8–10 randomly collected sub-samples that included loose soil in exposed areas) were collected using a manual corer during November 2018- October 2019. Soil samples from exposed stream banks were obtained from both bank profiles at any sampling site and, here, sub-samples from 6 to 8 such profiles were composited. All catchment source material samples were freeze dried, milled, and sieved using a 63 μm mesh.

2.3. Carbon and nitrogen content and bulk stable isotope ratio analyses

Source soil pH was measured at a 1:2.5 soil (dry) to water ratio before carbon (C) and nitrogen (N) stable isotope analysis. Soil and sediment samples were weighed into tin capsules and analysed using a Carlo Erba NA2000 elemental analyser (CE Instruments, Wigan, UK) interfaced with a PDZ Europa 20–22 isotope ratio mass spectrometer (SerCon Ltd., Crewe, UK). The isotopic results were expressed as natural abundance (δ) in parts per mil (‰) compared to international standards. The elemental and isotopic reference standard was IAR001 (wheat flour from Iso-Analytical, calibrated against IAEA-N-1 and IAEA-CH6:%N = 1.79%;%C = 40.46%; $\delta^{15}N$ = 2.51%; $\delta^{13}C$= - 25.99%). The analytical precision for elemental and isotopic reference standards was 0.42% and 0.2‰ for C and 0.03% and 0.2‰ for N, respectively.

2.4. Biotracer extraction and quantification

Total free lipids were extracted from soil and sediment samples (~12 g, spiked with FA C_{19} and alkane C_{34}) with dichloromethane:methanol

(9:1) using accelerated solvent extraction (Dionex 350) with three extraction cycles at 100 °C. Further details for the FA purification are reported in Upadhayay et al. (2020). To obtain the hydrocarbon fraction containing alkanes, the neutral lipid fraction was blown down to dryness with N_2 and redissolved in 2 ml hexane. The samples were eluted through silica gel using 6 ml hexane and then blown down to dryness with N_2. Finally, the samples were redissolved in 1 ml hexane for analyses.

Hydrolysable FAs were released from solvent extracted residues (~1 g; spiking with C_{19} FA) by treatment with 0.5 M KOH in methanol: water (9:1; 100 °C for 2 h) using a reflux method. The supernatant solution was recovered after centrifugation and the residue washed twice with a dichloromethane: methanol (9:1, v:v) mixture while extracts were combined. To obtain BFAs, the solution was adjusted to <2 pH with 6 M HCL. The aqueous solution was finally extracted with dichloromethane (3 times 2 ml). The volume of recombined extract was reduced under nitrogen. FAs were methylated with 14% BF_3 in methanol at 70 °C for 30 min.

The concentrations of alkanes were quantified using an Agilent 7890A GC with a flame ionization detector (FID) while FA (free and bound) concentrations were determined using an Agilent 6890 N/5973 N GC Mass Spectrometer (MS). Instrumental setup parameters are given in Table S1. The alkanes and FAs were identified by retention times, distinctive odd/even patterns and their characteristic mass spectrums and were quantified against the C_{34} alkane and C_{19} FA internal standard, respectively.

The compound-specific $\delta^{13}C$ signatures of alkanes, FFAs and BFAs were determined using a Finnigan Mat 6890 GC coupled to a Finnigan Mat Delta Plus IRMS via a Combustion III interface, with oxidation reactor containing platinum/copper oxide and nickel oxide at 940 °C (Thermo Fisher Scientific, Bremen, Germany). The $\delta^{13}C$ ratio was determined relative to CO_2 reference gas of known $\delta^{13}C$ and N5.5 grade purity (BOC, Guildford, UK) previously calibrated by Iso-Analytical (Crewe, UK). The reference gas was injected directly to the source just prior to the alkane and FA peaks of interest, and four times at the beginning and end of each run. The $\delta^{13}C$ was expressed relative to Vienna Pee Dee Belemnite (VPDB). During the runs, alkane and FA compound mixtures B4 and F8–3, with known $\delta^{13}C$ values (Indianna State University, US), were also analysed. The $\delta^{13}C$ values of FAs were corrected for the contribution of $\delta^{13}C$ values of the added methyl group during derivatisation. The stability and linearity of the system were better than 0.06‰. The $\delta^{13}C$ standard deviation from the standards was ± 0.35‰.

2.5. Estimation of field scale sediment loads

In order to evaluate the impact of land use change and/or heavy rainfall on soil erosion on pasture and arable land, two hydrologically-isolated fields (14 and 15) within the Cocktree catchment were used (Fig. 1a) due to their proximity and hydrological data availability. These fields are a part of the North Wyke Farm Platform (NWFP) which was established to test the sustainability of sheep and beef grazing systems (Orr et al., 2016). Field 14 (1.72 ha, slope range 1.7–2.5°) belongs to the so-called blue treatment (high sugar grass and white clover mix) and field 15 (1.54 ha, slope range 2.5–2.9°) belongs to the so-called red treatment (high sugar grass). Both fields were ploughed and reseeded in autumn 2017 and broadly represent the nature of local land use, especially pasture land, in the Cocktree study catchment. Field 14 remained grassland while field 15 was converted to arable land in August 2019 to grow winter wheat.

Flow and turbidity data for these fields for 2018 – 2020 were obtained from the NWFP portal (https://nwfp.rothamsted.ac. uk/). Turbidity was converted to suspended sediment concentration using the calibration curve described in Pulley and Collins (2020). Sediment loads from the two fields were estimated using the Loads Tool (Marsh et al., 2006) for the two contrasting winters and indirectly validated the changes in catchment scale sediment source apportionment during the study period.

2.6. Data processing and mixing model formulation

The abundance ($\mu g g^{-1}$ soil) of long chain odd-number (C_{23}–C_{33}) alkanes and even-number (C_{22}–C_{32}) FFAs and BFAs and their stable C isotope composition in soil and sediment were considered in this study. Various indices were calculated including total alkanes (∑alk), FFAs (∑FFA) and BFAs (∑BFA), odd-over-even pattern (OEP) of alkanes, and even-over-odd pattern of FFAs and BFAs (Text S1). Statistical differences in bulk isotopes, indices, biotracer content and their isotope values in source and sediment samples were determined using analysis of variance (ANOVA) followed by a Tukey HSD test at $p = 0.05$. Correlations between biotracer content and bulk carbon and soil pH were assessed in biplots.

Linear discriminant analysis was used to assess the performance of biotracers in differentiating the potential sediment sources. To estimate the relative contributions of sources to winter period sediment samples, long-chain alkane, FFA and BFA specific carbon stable isotope (in isolation or in combinations) and bulk isotope ($\delta^{13}C$ and $\delta^{15}N$) values of sources and sediments were used as tracers in a concentration-dependant Bayesian tracer mixing model (MixSIAR). A detailed description of MixSIAR used in our sediment source apportionment is included in Upadhayay et al. (2017) and its mathematical explanation is detailed in Stock et al. (2018). Because prolonged rainfall can lead to variations in soil erosion and hydrological connectivity, the winter period was used as a covariate incorporated via a fixed effect in the mixing model. Additionally, the MixSIAR framework was formulated with prior information on each source contribution to sediment yield (Text S2). Briefly, the potential median sediment loads from the individual catchment sediment sources were estimated (i.e., 80, 56, 40 and 1 tonne $year^{-1}$ for A, P, SB and W, respectively) based on the areal coverage of each land use/source and their reported field-based typical median soil erosion rates and used as a prior information in MixSIAR.

Despite potential alterations of isotope values during sediment redistribution (Upadhayay et al., 2021), we assumed such transformation occurred equally in all sources and used zero discrimination values in MixSIAR. The Markov Chain Monte Carlo (MCMC) parameters in MixSIAR were set as extreme (chain length = 3,000,000, burn = 1, 500,000, thin = 500, chains = 3). Convergence of model runs was checked using Gelman-Rubin and Geweke diagnostic statistics. Estimates of sediment source contributions based on the various biotracers were assessed using Hellinger distance based on Brown et al. (2018).

3. Results and discussion

3.1. Biogeochemical insights into sediment source discrimination

3.1.1. Bulk carbon and nitrogen properties

Organic carbon (OC) and total nitrogen (TN) contents were much higher in the woodland (7 ± 1.3%, 0.6 ± 0.1%) and pasture (5.1 ± 1.1%, 0.5 ± 0.1%) compared to arable and stream banks. The lower OC (2.3 ± 0.4%) and TN (0.3 ± 0.1%) ($p<0.001$) in arable soils were attributed to the interactions between tillage operations and low OC inputs into the soil. Continuous tillage practices and application of nitrogenous fertilizer can enhance degradation of soil organic matter as well as reduce cutin and suberin derived compounds in the soil (Man et al., 2021). Similar OC and TN contents in woodland and pasture soils suggested that pasture management has not had a significant negative impact on these soil characteristics.

Bulk C ($\delta^{13}C_{bulk}$) and N ($\delta^{15}N_{bulk}$) isotope values have been widely used to differentiate sediment sources and to trace biogeochemical cycling (Mahoney et al., 2019). The Cocktree catchment is dominated by C_3 vegetation and this was reflected in $\delta^{13}C_{bulk}$ values (−30.4 to −25.7‰) (Fig. 2). The $\delta^{13}C_{bulk}$ differentiated soil from arable (−27.7 ±

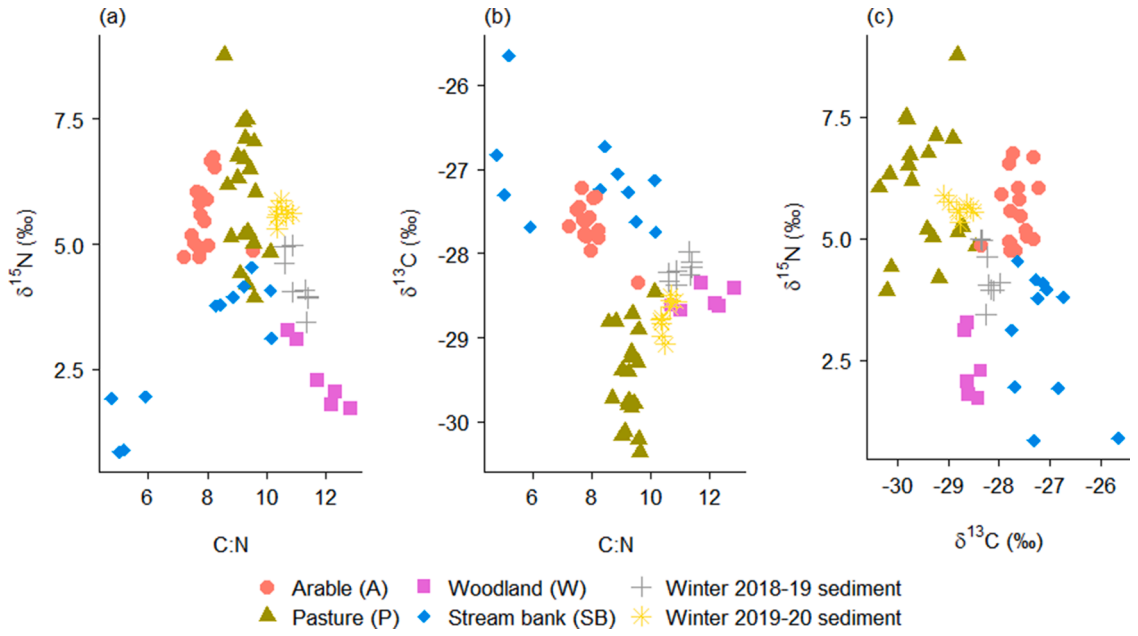

Fig. 2. Biplot of (a) $\delta^{15}N$ values and C:N ratios, (b) bulk $\delta^{13}C$ values and C:N ratios, and (c) bulk $\delta^{13}C$ and $\delta^{15}N$ values in source and sediment samples.

0.3‰) and pasture (−29.5 ± 0.6‰), whereas the $\delta^{15}N_{bulk}$ distinguished soil from pasture or arable vs stream banks or woodland (Fig. 2, Table 1). Differences also existed in the $\delta^{13}C_{bulk}$ and $\delta^{15}N_{bulk}$ values of pasture and stream bank sediment sources, but these did not differentiate arable vs stream banks or arable vs pasture. Higher $\delta^{15}N_{bulk}$ in arable and pasture soils suggested the influence of organic fertilizer applications and soil denitrification processes.

3.1.2. *Alkanes and FAs and their isotopic compositions*

Solvent extractable alkanes and FAs are a part of soil organic matter (Fig. 3a) derived from leaf wax and their variability, preservation and distribution depends on vegetation characteristics, soil properties and soil management (Jansen and Wiesenberg 2017). In arable soils, ∑Alk and ∑FFA ranged from 3.6 to 48.9 μg g^{-1} soil and 13 to 62.8 μg g^{-1}, respectively; representing 13–41% and 9–19% of the abundance found in woodland soil and 26–57% and 22–26% of the abundance found in pasture soils. These lipid compounds play a key role in soil aggregate stability (Lichtfouse et al., 1998) and the lower content suggests that arable soil is more vulnerable to erosion compared with the other land uses. Low alkane and FFA content in the arable soils was likely attributable to soil erosion, lower inputs from crops (removal of above ground biomass) as well as soil tillage facilitated mineralisation of these biotracers. Arable soil experiences significant perturbation during tillage operations which destroys the microaggregate fractions containing higher FFA content than the silt-clay fractions (Tamura et al., 2017).

Despite the marked variation in alkane and FFA contents, their abundance was within the reported range of agricultural, pasture, and forest soils (Li et al., 2018; Wiesenberg et al., 2004). The predominance of odd-carbon number alkanes (OEP >5) and even carbon-number FFAs (EOP >4) (Fig. 4) suggests these biotracers are derived from higher plants and are well preserved in these soils (except in stream banks) which is in common with the findings of Li et al. (2018). A significant higher OEP in pasture and woodland soils suggests lower decomposition of alkanes in these soils compared to arable land and stream banks. In contrast, the EOP of FFAs showed a relatively invariant pattern across the catchment sediment sources. The primary sources of long-chain alkanes and FFAs in soils have been shown to be leaf litter and farm yard manure (Bull et al., 2000; Upadhayay et al., 2020), and their preservation in the woodland topsoil might be due to a lower soil pH (4.9 ± 0.2) (Fig. 3b) because in acidic soils a strong association of FAs with soil minerals occurs due to ligand exchange (von Lützow et al. 2006). The significantly higher (~5 times) FFA content compared to alkanes in the soil samples (Fig. S2) agrees with the results of Wu et al. (2019), who found FAs can survive better during leaf litter degradation than alkanes. The highest FFA: alkane ratio (5.2 ± 2.7) in arable soils suggests that either FFA degradation is slower than that of alkanes or that the alkane input into arable soil is notably lower (Fig. S2). As land conversion has been shown to be associated with high alkane turnover rates in the first few years (Mendez-Millan et al., 2014), we posit that the FAs are better protected from biodegradation in soil. The net effect on the loss of soil organic matter and biotracer content is most likely explained by the stimulation of oxidation and exposure of the originally inaccessible organic compounds to attack by soil microorganisms due to tillage operations on the arable soils. The diagenetic alteration of biotracers leads to compositional changes; hence, biotracer composition does not provide robust information on the origin of sediment at catchment scale.

Different biotracers from the same land use have different $\delta^{13}C$ values, because of their biosynthetic pathways and spatial heterogeneity in soil hydrology (Reiffarth et al., 2016). Like $\delta^{13}C_{bulk}$ values, the ^{13}C signatures of the biotracers, including alkanes ($\delta^{13}C_{Alk;}$ −42.4 to −27.3‰) and FFAs ($\delta^{13}C_{FFA}$; −40.1 to −33.1‰), are in the reported range of soil under C3 vegetation (Diefendorf and Freimuth 2017; Upadhayay et al., 2020; Wiesenberg et al., 2004). The disconnection between $\delta^{13}C_{Alk}$ (e.g., C_{29}) and their biosynthetic precursor FAs (e.g., C_{30}) (Fig. S3, Table S2) within the same land use suggests the influence of multiple FA input sources and diagenetic fractionation processes in the soil (Fang et al., 2014; Lichtfouse 2012). Alkanes are biosynthesised during the brief period of leaf expansion while for FAs this occurs throughout the entire growing season (Freimuth et al., 2017). Consequently, the hydro-edaphic conditions of a specific time of the year can be imprinted on the $\delta^{13}C_{Alk}$ values, whereas $\delta^{13}C_{FFA}$ values are more representative of year-round hydro-edaphic variations in the soil system in addition to biosynthetic variations in plants and variations in diagenetic processes. In short, these biotracers constantly undergo diagenesis in the soil which can impact on ^{13}C-enrichment and thereby variation in the $\delta^{13}C$ values within a given sediment source. These controls explain the higher variability in $\delta^{13}C_{FFA}$ values compared with the other biotracers measured, irrespective of sediment source. Long-chain biotracers are produced by organisms other than plants in trace amounts (Dinel et al., 1990) and thus these biotracer isotopic values have potential for

Table 1
Biotracer isotopic compositions (‰) of potential sediment sources. Values within a row followed by the same superscript lower case letter are not statistically significantly different (***<0.001, **<0.01, *<0.05, ns = not significant).

	Biotracers	Arable (n = 17)	Pasture (n = 19)	Stream banks (n = 11)	Woodland (n = 6)
Bulk	$\delta^{15}N$***	5.5 ± 0.7^{bc}	6.0 ± 1.3^{c}	3.0 ± 1.3^{a}	2.4 ± 0.7^{a}
	$\delta^{13}C$***	−27.7 ± 0.3^{cd}	−29.5 ± 0. 6^{a}	−27.1 ± 0.6^{d}	−28.5 ± 0.1^{b}
Alkanes	$\delta^{13}C_{23}$*	−32.1 ± 2.3^{b}	−34.4 ± 2.4^{a}	−31.7 ± 2.3^{b}	−32.9 ± 1.5^{ab}
	$\delta^{13}C_{25}$***	−32.5 ± 1.5^{b}	−34.6 ± 2.3^{a}	−30.9 ± 1.3^{b}	−33.2 ± 1.3^{ab}
	$\delta^{13}C_{27}$***	−33.7 ± 1.1^{b}	−35.4 ± 2.0^{a}	−31.6 ± 0.8^{c}	−33.0 ± 0.6^{bc}
	$\delta^{13}C_{29}$***	−36.4 ± 1.2^{ab}	−37.9 ± 2.0^{a}	−33.9 ± 1.3^{c}	−35.1 ± 0.4^{bc}
	$\delta^{13}C_{31}$***	−36.6 ± 1.1^{ab}	−37.6 ± 1.9^{a}	−35.0 ± 1.0^{c}	−35.5 ± 0.7^{bc}
	$\delta^{13}C_{33}$***	−36.5 ± 1.6^{ab}	−37.7 ± 2.0^{a}	−35.1 ± 1.4^{b}	−34.9 ± 2.1^{b}
FFAs	$\delta^{13}C_{22}$***	−35.9 ± 0.8^{ab}	−36.5 ± 1.1^{a}	−34.5 ± 1.2^{c}	−34.9 ± 0.6^{bc}
	$\delta^{13}C_{24}$***	−35.7 ± 0.5^{bc}	−36.6 ± 1.0^{a}	−34.5 ± 1.1^{d}	−34.7 ± 0.6^{cd}
	$\delta^{13}C_{26}$***	−36.5 ± 1.0^{a}	−36.5 ± 0.9^{a}	−34.5 ± 1.0^{b}	−34.7 ± 0.5^{b}
	$\delta^{13}C_{28}$***	−36.6 ± 0.9$_{a}$	−37.0 ± 1.0^{a}	−34.7 ± 1.0^{b}	−35.0 ± 0.5^{b}
	$\delta^{13}C_{30}$***	−37.3 ± 0.8^{ab}	−37.7 ± 0.9^{a}	−35.6 ± 1.1^{c}	−36.3 ± 0.7^{bc}
	$\delta^{13}C_{32}$ns	−37.9 ± 1.2	−38.3 ± 0.7	−37.4 ± 1.4	−37.4 ± 1.0
BFAs	$\delta^{13}C_{22}$***	−33.5 ± 1.1^{ab}	−34.3 ± 0.8^{a}	−32.6 ± 1.4^{b}	−33.3 ± 1.2^{ab}
	$\delta^{13}C_{24}$**	−34.7 ± 1.4^{ab}	−34.9 ± 1.7^{a}	−33.2 ± 2.2^{b}	−34.6 ± 0.7^{ab}
	$\delta^{13}C_{26}$***	−35.9 ± 1.2^{ac}	−37.0 ± 1.4^{a}	−35.2 ± 1.1^{bc}	−34.6 ± 0.5^{c}
	$\delta^{13}C_{28}$ns	−35.4 ± 1.5	−36.4 ± 1.2	−35.5 ± 1.7	−34.6 ± 1.6
	$\delta^{13}C_{30}$ns	−36.0 ± 1.4	−36.0 ± 1.0	−35.5 ± 1.5	−35.5 ± 0.9
	$\delta^{13}C_{32}$*	−31.1 ± 1.0^{b}	−32.6 ± 1.0^{a}	−32.9 ± 2.8^{a}	−31.5 ± 0.7^{ab}

land use differentiation.

Robust sediment source discrimination using tracers is critically important for reliable estimation of sediment sources (Collins et al., 2020). In this study, good separation of sediment sources was achieved using the alkane, FFA and BFA isotope values (Table 1). Linear discriminant analysis indicated that $\delta^{13}C_{Alk}$ and $\delta^{13}C_{FFA}$ values can distinguish the potential sediment sources with reasonable accuracy (75% and 69%, respectively; Fig. S4). However, these tracers could not effectively distinguish arable vs pasture land probably due to the lack of significant inputs of biotracers to arable soil, the mixing of subsoil and topsoil during tillage and a legacy effect of previous crops/grass (Upadhayay et al., 2020). Notably, the inclusion of the bulk tracer values in the tracer set significantly improved the accuracy of sediment source discrimination to 96% (Fig. 5). However, river sediment $\delta^{13}C_{bulk}$ values can be biased towards riparian vegetation (Marwick et al., 2014) and $\delta^{15}N_{bulk}$ can transform unpredictably (Upadhayay et al., 2021) and hence should be used cautiously in sediment source apportionment modelling.

3.1.3. BFAs and isotope compositions

Like alkanes and FFAs, BFA abundance was significantly lower in the arable land. Arable soil ∑BFA ranged up to 7.9 to 31 μg g^{-1} soil (16–29% and 33–50% of the abundance found in woodland and pasture soils, respectively). The abundances of C_{22}, C_{24} and C_{26}, the main components of plant suberin (Feng et al., 2010), were relatively unaffected by microbial degradation in the woodland and pasture source soils. Long-chain BFAs in soil may experience intense microbial transformation of the vegetation-derived FAs of different quality, but they preserve in soil due to physico-chemical stabilisation processes. In soil, suberin can be an important source of BFAs due to its presence in root tissues (removal of above ground biomass) and relatively high resistance to biodegradation due to a high phenolic unit in its structure (Nierop et al., 2006). Lipids derived from roots may be degraded less than those derived from shoots (Nguyen Tu et al. 2020) and BFAs are considered good indicators of the inputs and degradation of cutin and suberin biopolymers.

The BFA carbon isotope values ($\delta^{13}C_{BFA}$) were relatively enriched compared to $\delta^{13}C_{FFA}$ homologues and ranged from −39.5 to −26.8‰. Larger isotopic differences occurred in C_{32} homologues, regardless of sediment source, while $\delta^{13}C_{BFA}$ values in arable soil were higher compared to FFAs regardless of carbon-chain length. Clear enrichment of ^{13}C in BFAs compared to FFAs in arable soils and stream banks regardless of chain length (Table 1) implies that the arable soil contains highly processed BFAs. Differences between the FFAs and BFAs suggests that diagenetic and heterotrophic reworking processes can significantly change long-chain $\delta^{13}C_{FFA}$ values in soil. In line with our results, Yang et al. (2020) found increasing FA stability with decreasing C chain length. Physical protection in soil aggregates (Wiesenberg et al., 2010) as well as encapsulation within larger organic micro-molecules (Lichtfouse 2012) can protect alkane and FA in soil from soil microbial degradation. In general, enrichment of $\delta^{13}C_{BFA}$ compared to $\delta^{13}C_{FFA}$ might be related to: 1) contribution from root tissues (e.g., suberin); 2) microbial decomposition of FFAs, and; 3) addition of microbial necromass. BFAs provided good discrimination amongst the sampled sources (Fig. 5c, Fig. S4c) reflecting the fact that these biotracers are considered more diagnostic for subsoil sources (e.g., stream banks in our case) than the FFAs (Feng et al., 2010; Nierop et al., 2006) despite the latter being regarded as having more powerful fingerprinting potential for land use sources due to a direct link with overlaying vegetation composition.

3.2. Progress in sediment source apportionment using different biotracers

Our work provided an opportunity to assess the utility of different biotracers for sediment source apportionment. The biotracers unanimously suggested that the contribution of stream banks to winter 2018–19 sediment samples was high, but the corresponding contributions to winter 2019–20 sediment differed depending on the biotracers (Fig. 6). Alkane-based estimation suggested similar stream bank contributions (~36%) to both winter period sediments with arable (34%) in winter 2018–19 and pasture (34%) in winter 2019–20 as the second most important sources. Although the alkanes provided good source discrimination (Fig. 5a, Fig. S4a), mixing model performance was poor and the precision of the estimated source proportions was lower (wider credible intervals) than using the other biotracers (Fig. 6). The $\delta^{13}C_{Alk}$ data exhibited less influence on the estimated sediment source contributions (hellinger distance close to zero, Table S3) compared to $\delta^{13}C_{FFA}$ and $\delta^{13}C_{BFA}$. Both FFAs and BFAs returned similar information on the source contributions in winter 2018–19, with the highest contribution from stream banks (76% and 71%, respectively). For winter 2019–20 sediment, however, FFA-based estimation suggested that stream banks were still the primary sediment source (66%) whereas, BFA-based estimation indicated that almost half (52%) of the sampled sediment was derived from arable land. Despite the relatively high stream bank contributions estimated by BFAs and FFAs compared to other studies (e.g., up to 55%; Evans et al., 2017), BFAs were judged to provide more realistic information based on field observations (Fig. 1c), narrow credible intervals and a hellinger distance close to 1.

Notably, the choice of biotracers and mixing model structure can significantly impact on the accuracy and precision of estimated sediment

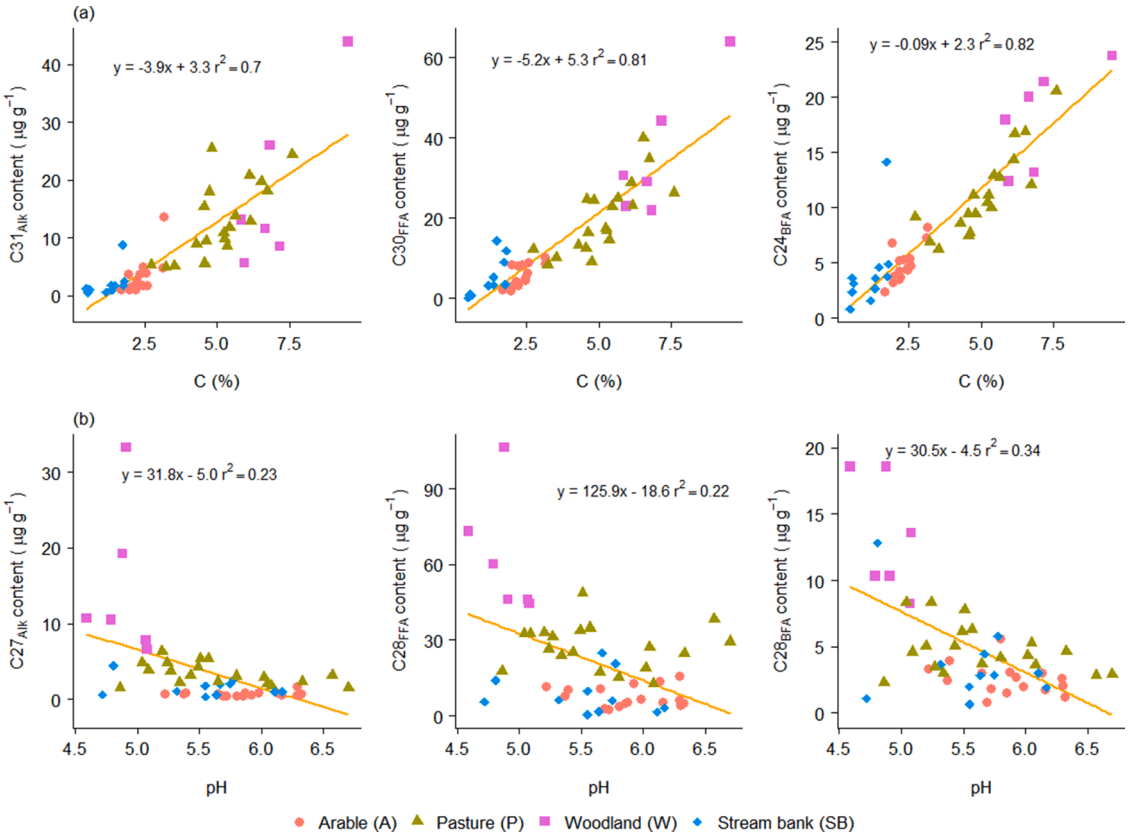

Fig. 3. Relationships between biotracer content with (a) OC and (b) soil pH.

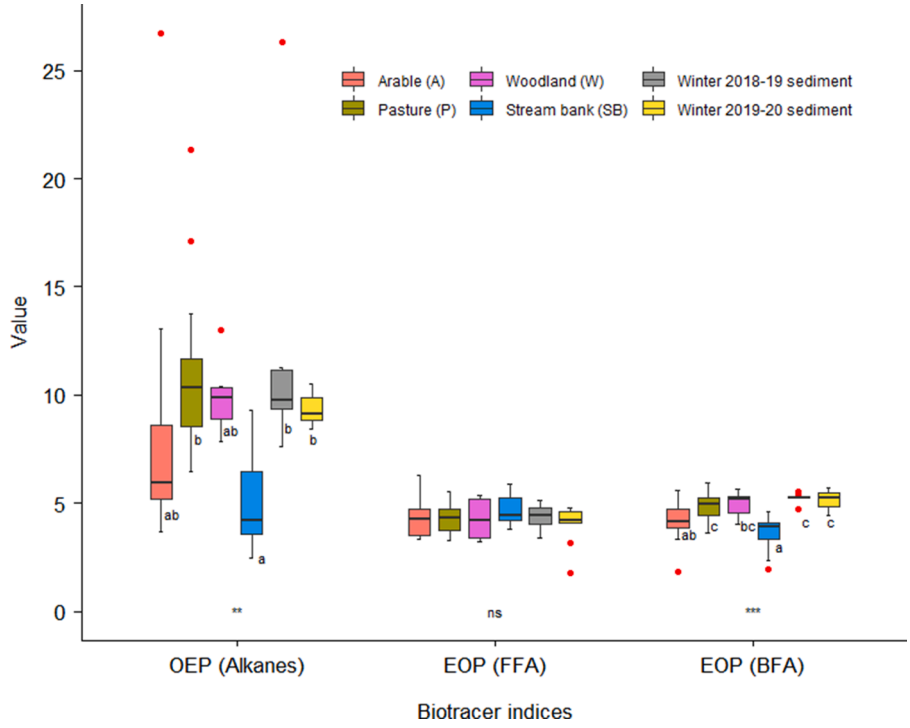

Fig. 4. Distribution of odd-over-even pattern (OEP) and even-over-odd pattern (EOP) of biotracers in soil and sediment samples. Similar letters within a biotracer indicate no statistically significant difference across the sources and sediments. Red dots indicate outliers. Asterisks indicate significance levels (ns = not significant, ** = <0.01 and *** = <0.001).

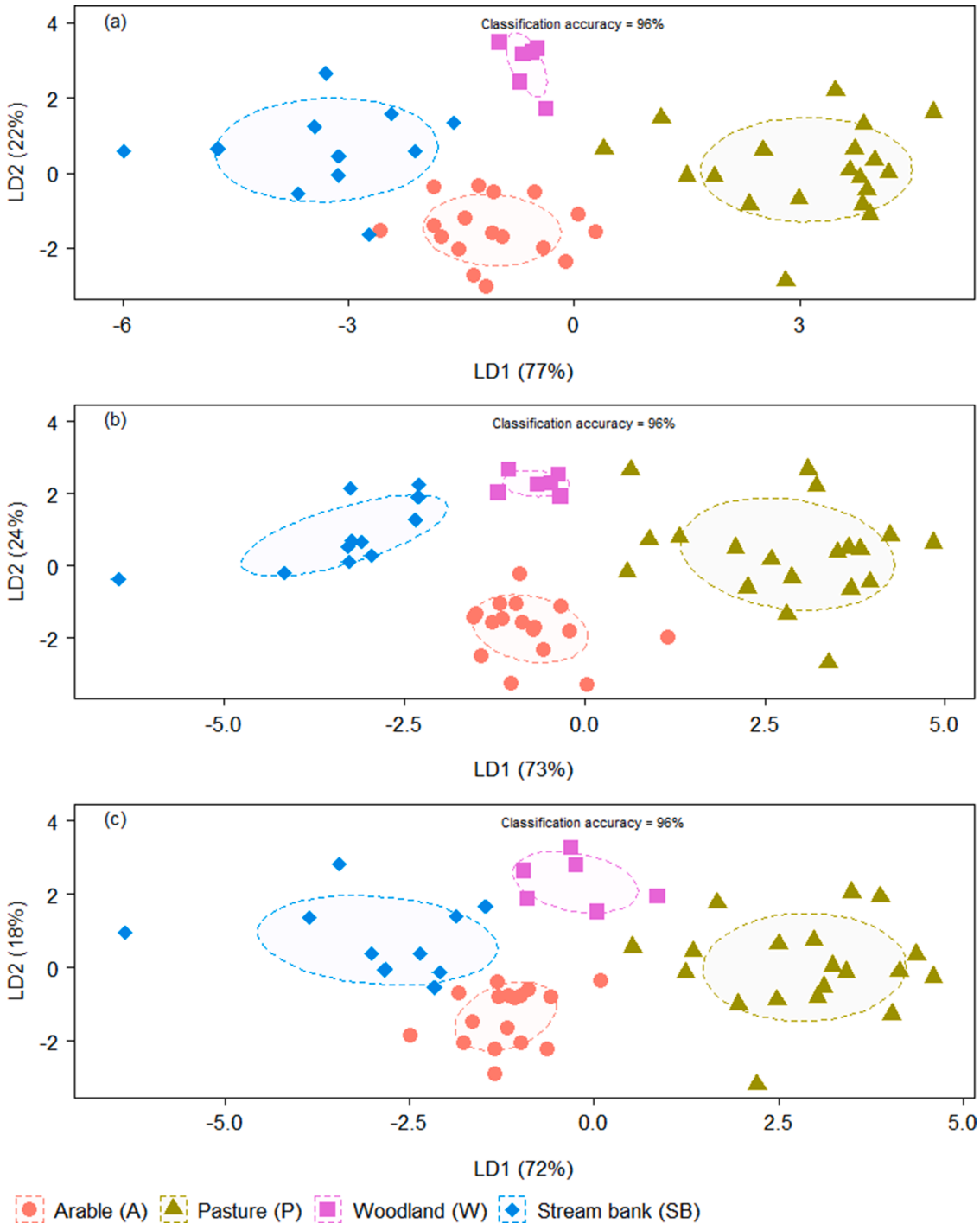

Fig. 5. Linear discriminant analysis of carbon isotopes of (a) alkanes, (b) FFAs and (c) BFAs in combination with bulk isotopes of C and N in potential sediment sources. Ellipses are drawn on 50% confidence limits.

source contributions (Fig. 6, Fig. S5). Composite fingerprints involving various biotracers can be highly promising for the apportionment of sediment sources that cannot be distinguished using other commonly used geochemical tracers in a catchment with complex land use. To the best of our knowledge, no previous study has characterized long-chain alkane, FFA and BFA abundance and corresponding $\delta^{13}C$ values at catchment scale for apportioning sediment sources quantitatively.

The ways in which biotracers move through river catchments can cause their transformation which is of critical importance for sediment source apportionment. Physical, chemical and biological factors can change during sediment transport leading to enchanced decomposition and mineralisation of biotracers within sediment (de Nijs and Commeraat, 2020; Xiao et al., 2018) and thereby alteration of the original isotopic composition inherited from the contributing sources (Upadhayay et al., 2021). The contrasting sediment source composition estimated using the different biotracers (Fig. 6), indicated that alkanes were not sensitive enough to apportion sediment sources correctly. In fact, alkanes cannot form strong bonds with soil and sediment due to their non-functionalised apolar nature, meaning that these biotracers are mostly protected by being enclosed within the intracellular space of clay minerals (e.g., montmorillonite; Eltantawy and Arnold (1972)). This issue could be used to make an informed decision to reject alkanes as a

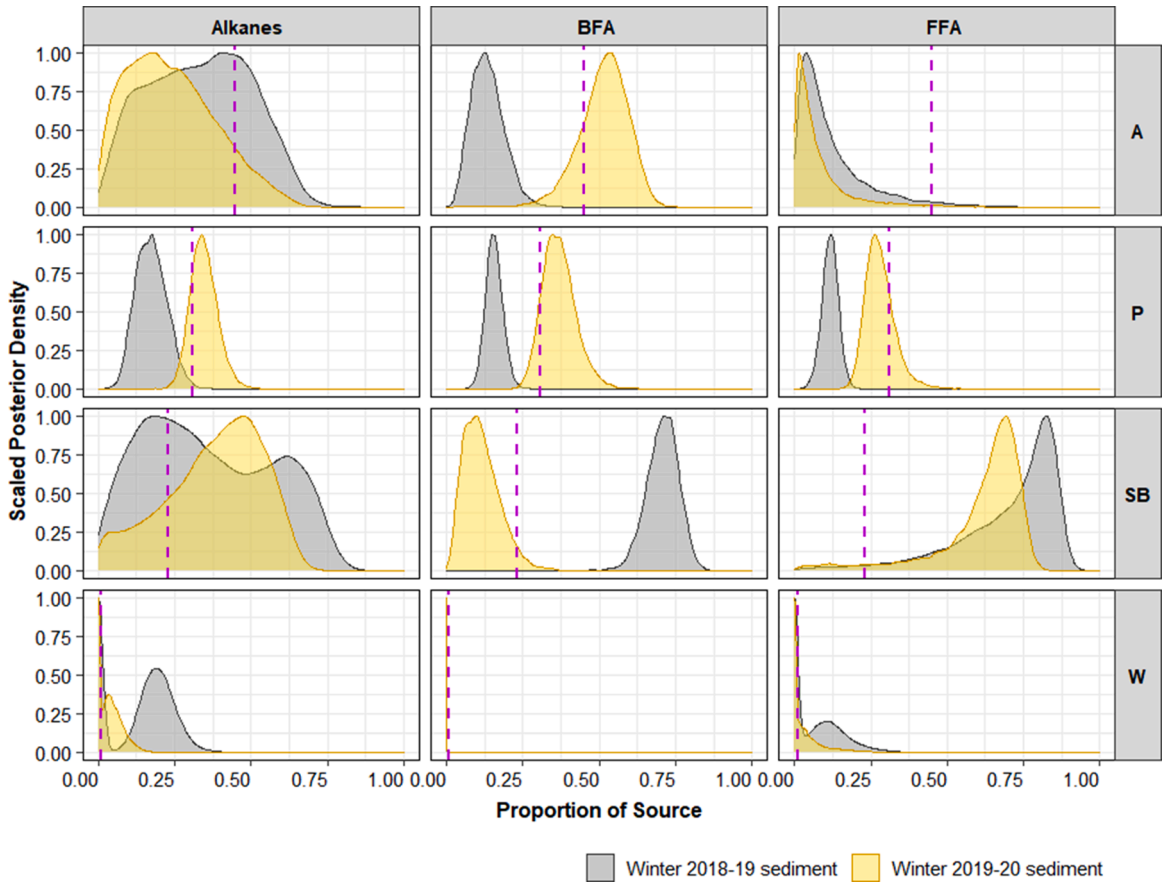

Fig. 6. Sediment source (A = arable, P = pasture, SB = stream banks and W = woodland) apportionment for the winter 2018–19 and winter 2019–20 sediment samples using long-chain alkane, FFA (free fatty acid) and BFA (bound fatty acid) isotopic values in combination with bulk isotopes of C and N. Vertical dotted line indicates prior information.

robust biotracer for sediment source apportionment. In contrast, FAs, due to their mode of occurrence (entrapment in microaggregates and direct organo-mineral association), preferentially remain (>50%) in the silt and clay size fraction (Angst et al., 2018) and are less likely to be disturbed by aggregate breakdown during erosion. Because of this, fine sediment sources in our study catchment were better represented by BFAs. Nevertheless, many processes can complicate the interpretation of any biotracer signatures in sediment. These include selective leaching of alkanes or FAs from plant litter and soils (Jandl et al., 2013), leaf wax inputs from direct litter fall (Freimuth et al., 2019), dry deposition of

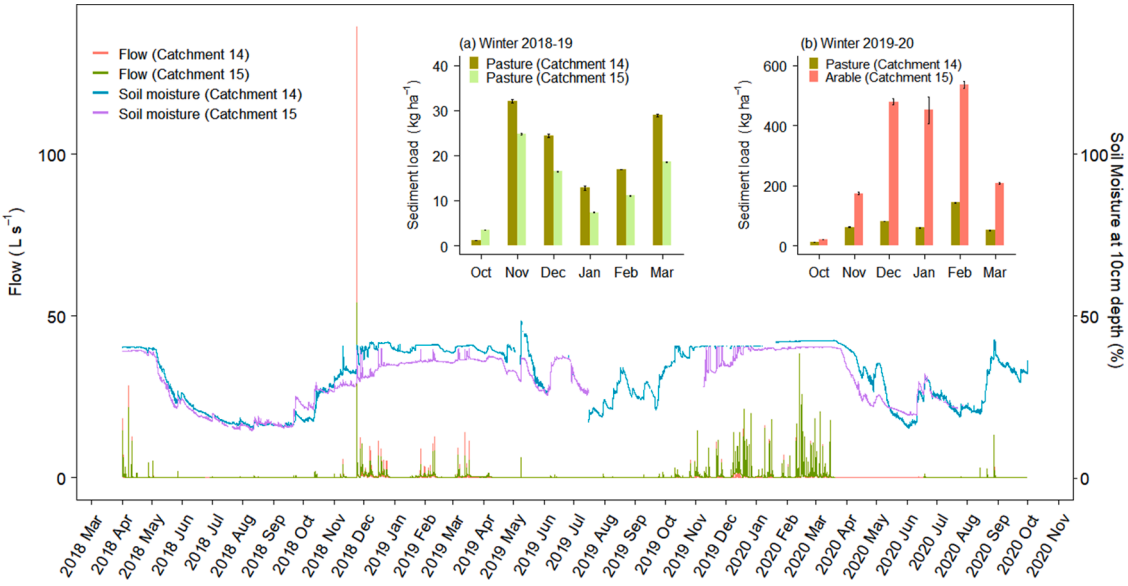

Fig. 7. Flow and soil moisture of the North Wyke Farm Platform field scale catchments 14 and 15 (see Fig. 1 for location) with sediment loads for (a) winter 2018–19 and (b) winter 2019–20. Catchment 14 remained grassland throughout the study period, while catchment 15 was ploughed in August 2019 to grow winter wheat.

particulate waxes (Nelson et al., 2018) or sorption/desorption of biotracers in transit. Additionally, the efficiency of time-integrated sediment samplers for retaining very fine sediment during different flow conditions may introduce some degree of uncertainty in biotracer values. It is not clear at this stage to what extent these processes introduce uncertainties in sediment source estimates and further research is certainly warranted here.

3.3. Land use change as a dominant driver of sediment dynamics during an extreme wet winter

The magnitude of sediment flux is influenced by the intricate interactions between land use management and rainfall. Unsurprisingly, arable land erosion was expected to be an important source of sediment in the extreme wet winter (Fig. 6) given the relatively steep slopes (median 4.5°), exposure of bare tilled soils to erosive rainfall (Fig. 1c) as well as the role of conventional tillage practices for winter cereals in degrading soil structure and enhancing surface-water runoff (Palmer and Smith 2013). Importantly, the increase in arable land contributions during winter 2019–20 at the catchment outlet is strongly supported by field scale sediment load data from the NWFP that showed sediment loss from arable land was ~4.6 times higher than that from adjacent pasture land (Fig. 7b). This increase is explicitly attributed to the impact of land use conversion from grassland to arable land. It should be noted that field 15 on the NWFP was new arable land which may not be fully representative of longer-term arable land in the study catchment. It is plausible that long-term arable land can produce higher loss of sediment than arable land freshly converted from non-marginal land due to higher compaction, lower organic matter content and higher destruction of soil aggregates during long-term tillage operations. Extreme rainfall alone in winter 2019–20 contributed a ~3.5 times increase in sediment loss from pasture at field scale (Fig. 7b) despite the absence of grazing animals for most of the study months. This is attributed to heavy rainfall increasing topsoil erosion and overland flow transport following strong establishment of surface pathway connectivity. Here, our field scale data can be interpreted alongside the 'best guess' of Favis-Mortlock and Boardman (1995) who suggested a 10% increase in winter rainfall could trigger a 150% increase in annual water erosion. Our data are in line with other studies both in the UK and around the world reporting that agricultural activities and land conversion to arable production are responsible for accelerated soil erosion (Evans et al., 2017; Prăvălie et al., 2021) and that extreme rainfall increases erosion and sediment delivery even from land with recommended best management practices (Fiener et al., 2019).

Although field 14 was assumed to represent the majority of pasture land in the study catchment, it should be noted that our monitored field scale sediment loads on the NWFP may not be fully representative of the sediment loads from pasture or arable land in the study catchment due to variations in rainfall, topography, field size, tillage intensity, surface cover and sediment connectivity. Here, it is noteworthy that substantial variability in rainfall and sediment loads amongst the NWFP field scale catchments has been reported by previous work (Zhang et al., 2022; Pulley and Collins, 2020). Nevertheless, our field scale data provided first-hand information on the impact of heavy rainfall and/or land use change on soil erosion for helping to corroborate the corresponding source contributions at larger scale. We do acknowledge, nonetheless, that extrapolation of field scale data is challenged by the intrinsic variability and non-linearity of erosion and sediment transport processes across scales (Kirkels et al., 2014).

Rainfall amount is widely recognised as an important driver for runoff and sediment export at landscape scale (Baartman et al., 2020). Our study showed that the elevated low and high rain days (35%, 55% and 50% more days with >1 mm, >5 mm, >20 mm rainfall respectively; Fig. 1b) in winter 2019–20 compared with winter 2018–19, most likely enhanced sediment loss from pasture and arable land. This can be attributed to a significant increase in saturation driven surface runoff as a result of prolonged low-intensity rainfall (Fig. S6), because antecedent soil hydrological conditions (e.g. soil moisture content ~50% in arable and pasture field, Fig. 7) are an important control for hydro-sedimentological responses (McMillan et al., 2018). The catchment scale increase in pasture source contributions in winter 2019–20, compared to winter 2018–19, was about 1 order of magnitude lower than the corresponding monitored field scale increase in sediment load. This clearly demonstrated that even well-managed pasture is not resistance to the prolonged rainfall in terms of sediment loss and this can certainly increase sediment flux at the catchment scale. Disentangling the combined effects of prolonged rainfall and agricultural activities in increasing or decreasing sediment source contributions at the catchment scale is not straight forward. Nevertheless, our field scale sediment loss monitoring on the NWFP provided a blueprint that heavy rainfall and land use interact non-linearly and that their combined impact is highly detrimental (the catchment 15 erosion rate increased ~23 times in winter 2019–20 compared with winter 2018–19) to water and soil security.

4. Conclusions

Interactions between prolonged heavy rainfall and land use can elevate sediment loss and, in turn, this can undermine the efficacy of current best management practices for delivering sustainable agricultural intensification. Using and contrasting multiple biotracers in a fingerprinting procedure, backed up by field scale monitoring of sediment loss from pasture and arable land on the one of the worlds most instrumented farm platforms, our work shows a significant shift in both field scale erosion rates and catchment sediment source contributions during the 'wet' winter 2019–20, compared to the relatively 'dry' winter 2018–19. This shift underscores the current lack of resistance to 'perfect storms' of extreme wet weather and land use risks in our lowland farmed landscapes in the UK. Effective transition of the UK's agricultural sector to help deliver more public goods and services clearly requires greater resilience to abiotic (and indeed biotic) stresses including those studied in this paper. Given projections of climate change, some recent land use modelling (Ritchie et al., 2019) suggests an expansion of the area under erosion prone crops (e.g., cereals) in our study area and the surrounding region of SW England. Our findings herein underscore the likely risk of significant environmental impacts under such scenarios unless the buffering capacity and resistance of agricultural landscapes is improved significantly. Clearly, long-term application of the approaches reported in this paper provide a robust means to monitor the impacts of any coordinated strategies to address the lack of resistance across scales. Through our application of multiple biotracers in the source fingerprinting component of the work herein, we recommend the use of FAs and especially BFAs for source apportionment, rather than alkanes. Further work is needed to test the conservative behaviour of the biotracers applied in this study and that work could include edge-of-field analysis using the NWFP infrastructure.

Declaration of Competing interest

The authors declare that they have no known competing financial interests or personal relationships that could have appeared to influence the work reported in this paper.

Acknowledgements

This work was funded by the UKRI-BBSRC (UK Research and Innovation-Biotechnology and Biological Sciences Research Council) via grant award BBS/E/C/000I0330. We would like to thank three anonymous reviewers for their insightful comments on this work.

Supplementary materials

Supplementary material associated with this article can be found, in the online version, at doi:10.1016/j.watres.2022.118348.

References

Angst, G., Nierop, K.G.J., Angst, S., Frouz, J., 2018. Abundance of lipids in differently sized aggregates depends on their chemical composition. Biogeochemistry 140 (1), 111–125.

Baartman, J.E.M., Nunes, J.P., Masselink, R., Darboux, F., Bielders, C., Degre, A., Cantreul, V., Cerdan, O., Grangeon, T., Fiener, P., Wilken, F., Schindewolf, M., Wainwright, J., 2020. What do models tell us about water and sediment connectivity? Geomorphology, 107300.

Borrelli, P., Robinson, D.A., Panagos, P., Lugato, E., Yang, J.E., Alewell, C., Wuepper, D., Montanarella, L., Ballabio, C., 2020. Land use and climate change impacts on global soil erosion by water (2015-2070). In: Proceedings of the National Academy of Sciences, 202001403.

Brown, C.J., Brett, M.T., Adame, M.F., Stewart-Koster, B., Bunn, S.E., 2018. Quantifying learning in biotracer studies. Oecologia 187 (3), 597–608.

Bull, I.D., Bergen, P.F.v., Nott, C.J., Poulton, P.R., Evershed, R.P., 2000. Organic geochemical studies of soils from the Rothamsted classical experiments V. The fate of lipids in different long-term experiments. Org. Geochem. 31 (5), 389–408.

Collins, A.L., Blackwell, M., Boeckx, P., Chivers, C.-.A., Emelko, M., Evrard, O., Foster, I., Gellis, A., Gholami, H., Granger, S., Harris, P., Horowitz, A.J., Laceby, J.P., Martinez-Carreras, N., Minella, J., Mol, L., Nosrati, K., Pulley, S., Silins, U., da Silva, Y.J., Stone, M., Tiecher, T., Upadhayay, H.R., Zhang, Y., 2020. Sediment source fingerprinting: benchmarking recent outputs, remaining challenges and emerging themes. J. Soils Sed. 20 (12), 4160–4193.

de Nijs, E.A., Cammeraat, E.L.H., 2020. The stability and fate of soil organic carbon during the transport phase of soil erosion. Earth-Sci. Rev. 201, 103067.

Diefendorf, A.F., Freimuth, E.J., 2017. Extracting the most from terrestrial plant-derived n-alkyl lipids and their carbon isotopes from the sedimentary record: a review. Org. Geochem. 103, 1–21.

Dinel, H., Schnitzer, M., Mehuys, G., ,1990. Soil lipids: origin, nature, content, decompostion, and effect on soil physical properties. In: Bollag, J.M., Stotzky, G. (Eds.), Soil Biochemistry. Marcel Dekker Inc, New York, pp. 379–429.

Eltantawy, I.M., Arnold, P.W., 1972. Adsorption of n-alkanes by Wyoming montmorillonite. Nature Phys. Sci. 237 (77), 123–125.

Evans, R., Collins, A.L., Zhang, Y., Foster, I.D.L., Boardman, J., Sint, H., Lee, M.R.F., Griffith, B.A., 2017. A comparison of conventional and ^{137}Cs-based estimates of soil erosion rates on arable and grassland across lowland England and Wales. Earth-Sci. Rev. 173, 49–64.

Fang, J., Wu, F., Xiong, Y., Li, F., Du, X., An, D., Wang, L, 2014. Source characterization of sedimentary organic matter using molecular and stable carbon isotopic composition of n-alkanes and fatty acids in sediment core from Lake Dianchi. China. Sci. Total Environ. 473-474, 410–421.

Favis-Mortlock, D., Boardman, J., 1995. Nonlinear responses of soil erosion to climate change: a modelling study on the UK South Downs. Catena 25 (1), 365–387.

Feng, X., Gustafsson, Ö., Holmes, R.M., Vonk, J.E., van Dongen, B.E., Semiletov, I.P., Dudarev, O.V., Yunker, M.B., Macdonald, R.W., Wacker, L., Montluçon, D.B., Eglinton, T.I., 2015. Multimolecular tracers of terrestrial carbon transfer across the pan-Arctic: ^{14}C characteristics of sedimentary carbon components and their environmental controls. Global Biogeochem. Cycles 29 (11), 1855–1873.

Feng, X.J., Xu, Y.P., Jaffe, R., Schlesinger, W.H., Simpson, M.J., 2010. Turnover rates of hydrolysable aliphatic lipids in Duke Forest soils determined by compound specific ^{13}C isotopic analysis. Org. Geochem. 41 (6), 573–579.

Fiener, P., Wilken, F., Auerswald, K., 2019. Filling the gap between plot and landscape scale – eight years of soil erosion monitoring in 14 adjacent watersheds under soil conservation at Scheyern, Southern Germany. Adv. Geosci. 48, 31–48.

Freimuth, E.J., Diefendorf, A.F., Lowell, T.V., 2017. Hydrogen isotopes of n-alkanes and n-alkanoic acids as tracers of precipitation in a temperate forest and implications for paleorecords. Geochim. Cosmochim. Acta 206, 166–183.

Freimuth, E.J., Diefendorf, A.F., Lowell, T.V., Wiles, G.C., 2019. Sedimentary n-alkanes and n-alkanoic acids in a temperate bog are biased toward woody plants. Org. Geochem. 128, 94–107.

Jandl, G., Baum, C., Leinweber, P., 2013. Crop-specific differences in the concentrations of lipids in leachates from the root zone. Arch. Agron. Soil Sci. 59 (1), 119–125.

Jansen, B., Wiesenberg, G.L.B., 2017. Opportunities and limitations related to the application of plant-derived lipid molecular proxies in soil science. SOIL 3 (4), 211–234.

Kirkels, F.M.S.A., Cammeraat, L.H., Kuhn, N.J., 2014. The fate of soil organic carbon upon erosion, transport and deposition in agricultural landscapes — A review of different concepts. Geomorphology 226, 94–105.

Li, X., Anderson, B.J., Vogeler, I., Schwendenmann, L., 2018. Long-chain n-alkane and n-fatty acid characteristics in plants and soil - potential to separate plant growth forms, primary and secondary grasslands? Sci. Total Environ. 645, 1567–1578.

Li, Z., Fang, H., 2016. Impacts of climate change on water erosion: a review. Earth-Sci. Rev. 163, 94–117.

Lichtfouse, E., 2012. ^{13}C-dating, the first method to calculate the relative age of molecular substance homologues in soil. Environ. Chem. Lett. 10 (1), 97–103.

Lichtfouse, E., Wehrung, P., Albrecht, P., 1998. Plant wax n-alkanes trapped in soil humin by noncovalent bonds. Naturwissenschaften 85 (9), 449–452.

Mahoney, D.T., Al Aamery, N., Fox, J.F., Riddle, B., Ford, W., Wang, Y.T, 2019. Equilibrium sediment exchange in the earth's critical zone: evidence from sediment fingerprinting with stable isotopes and watershed modeling. J. Soils Sed. 19, 3332–3356.

Man, M., Deen, B., Dunfield, K.E., Wagner-Riddle, C., Simpson, M.J., 2021. Altered soil organic matter composition and degradation after a decade of nitrogen fertilization in a temperate agroecosystem. Agric. Ecosyst. Environ. 310, 107305.

Marsh, N., Steven, A., Tennakoon, S., Arene, S., Farthing, B., Fox, D, 2006. Loads Tool v1. 0.0 b. Queensland Environmental Protection Agency: Indooroopilly, Australia. QNRM06085.

Marwick, T.R., Borges, A.V., Van Acker, K., Darchambeau, F., Bouillon, S., 2014. Disproportionate contribution of riparian inputs to organic carbon pools in freshwater systems. Ecosystems 17 (6), 974–989.

McMillan, S.K., Wilson, H.F., Tague, C.L., Hanes, D.M., Inamdar, S., Karwan, D.L., Loecke, T., Morrison, J., Murphy, S.F., Vidon, P., 2018. Before the storm: antecedent conditions as regulators of hydrologic and biogeochemical response to extreme climate events. Biogeochemistry 141 (3), 487–501.

Mendez-Millan, M., Nguyen Tu, T.T., Balesdent, J., Derenne, S., Derrien, D., Egasse, C., Thongo, M., Bou, A., Zeller, B., Hatté, C.J.B., 2014. Compound-specific ^{13}C and ^{14}C measurements improve the understanding of soil organic matter dynamics. Biogeochemistry 118 (1), 205–223.

Nelson, D.B., Ladd, S.N., Schubert, C.J., Kahmen, A., 2018. Rapid atmospheric transport and large-scale deposition of recently synthesized plant waxes. Geochim. Cosmochim. Acta 222, 599–617.

Nguyen Tu, T.T., Vidal, A., Quénéa, K., Mendez-Millan, M., Derenne, S, 2020. Influence of earthworms on apolar lipid features in soils after 1 year of incubation. Biogeochemistry 147 (3), 243–258.

Nierop, K.G.J., Jansen, B., Hageman, J.A., Verstraten, J.M., 2006. The complementarity of extractable and ester-bound lipids in a soil profile under pine. Plant Soil 286 (1–2), 269–285.

Orr, R.J., Murray, P.J., Eyles, C.J., Blackwell, M.S.A., Cardenas, L.M., Collins, A.L., Dungait, J.A.J., Goulding, K.W.T., Griffith, B.A., Gurr, S.J., Harris, P., Hawkins, J.M. B., Misselbrook, T.H., Rawlings, C., Shepherd, A., Sint, H., Takahashi, T., Tozer, K.N., Whitmore, A.P., Wu, L., Lee, M.R.F., 2016. The north wyke farm platform: effect of temperate grassland farming systems on soil moisture contents, runoff and associated water quality dynamics. Eur. J. Soil Sci. 67 (4), 374–385.

Palmer, R.C., Smith, R.P., 2013. Soil structural degradation in SW England and its impact on surface-water runoff generation. Soil Use Manag. 29 (4), 567–575.

Phillips, J.M., Russell, M.A., Walling, D.E., 2000. Time-integrated sampling of fluvial suspended sediment: a simple methodology for small catchments. Hydrol. Process. 14 (14), 2589–2602.

Prăvălie, R., Patriche, C., Borrelli, P., Panagos, P., Roșca, B., Dumitrașcu, M., Nita, I.-A., Săvulescu, I., Birsan, M.-.V., Bandoc, G., 2021. Arable lands under the pressure of multiple land degradation processes. A global perspective. Environ. Res. 194, 110697.

Pulley, S., Collins, A.L., 2020. Sediment loss in response to scheduled pasture ploughing and reseeding: the importance of soil moisture content in controlling risk. Soil Till Res. 204, 104746.

Reiffarth, D.G., Petticrew, E.L., Owens, P.N., Lobb, D.A., 2016. Sources of variability in fatty acid (FA) biomarkers in the application of compound-specific stable isotopes (CSSIs) to soil and sediment fingerprinting and tracing: a review. Sci. Total Environ. 565, 8–27.

Ritchie, P.D.L., Harper, A.B., Smith, G.S., Kahana, R., Kendon, E.J., Lewis, H., Fezzi, C., Halleck-Vega, S., Boulton, C.A., Bateman, I.J., Lenton, T.M., 2019. Large changes in Great Britain's vegetation and agricultural land-use predicted under unmitigated climate change. Environ. Res. Lett. 14 (11), 114012.

Sartori, M., Philippidis, G., Ferrari, E., Borrelli, P., Lugato, E., Montanarella, L., Panagos, P., 2019. A linkage between the biophysical and the economic: assessing the global market impacts of soil erosion. Land Use Policy 86, 299–312.

Stock, B.C., Jackson, A.L., Ward, E.J., Parnell, A.C., Phillips, D.L., Semmens, B.X., 2018. Analyzing mixing systems using a new generation of Bayesian tracer mixing models. PeerJ 6, e5096.

Tamura, M., Suseela, V., Simpson, M., Powell, B., Tharayil, N., 2017. Plant litter chemistry alters the content and composition of organic carbon associated with soil mineral and aggregate fractions in invaded ecosystems. Global Change Biol. 23 (10), 4002–4018.

Tandon, A. and Schultz, A. (2020) Met office: the UK's wet and warm winter of 2019-20. https://www.carbonbrief.org/met-office-the-uks-wet-and-warm-winter-of-2019-20 (Access date: 23 Aug, 2020).

Tye, A.M., Rawlins, B.G., Rushton, J.C., Price, R., 2016. Understanding the controls on sediment-P interactions and dynamics along a non-tidal river system in a rural–urban catchment: the River Nene. Appl. Geochem. 66, 219–233.

Upadhayay, H.R., Bodé, S., Griepentrog, M., Huygens, D., Bajracharya, R.M., Blake, W. H., Dercon, G., Mabit, L., Gibbs, M., Semmens, B.X., Stock, B.C., Cornelis, W., Boeckx, P., 2017. Methodological perspectives on the application of compound-specific stable isotope fingerprinting for sediment source apportionment. J. Soils Sed. 17 (6), 1537–1553.

Upadhayay, H.R., Granger, S.J., Zhang, Y., Amorim, F., Cilione, L., Micale, M., Collins, A. L., 2021. Insights into bulk stable isotope alteration during sediment redistribution to edge-of-field: impact on sediment source apportionment. Biogeochemistry 155, 263–281.

Upadhayay, H.R., Griepentrog, M., Bodé, S., Bajracharya, R.M., Cornelis, W., Collins, A. L., Boeckx, P., 2020. Catchment-wide variations and biogeochemical time lags in soil fatty acid carbon isotope composition for different land uses: implications for sediment source classification. Org. Geochem. 146, 104048.

von Lützow, M., Kogel-Knabner, I., Ekschmitt, K., Matzner, E., Guggenberger, G., Marschner, B., Flessa, H., 2006. Stabilization of organic matter in temperate soils: mechanisms and their relevance under different soil conditions - a review. Eur. J. Soil Sci. 57 (4), 426–445.

Wiesenberg, G.L.B., Dorodnikov, M., Kuzyakov, Y., 2010. Source determination of lipids in bulk soil and soil density fractions after four years of wheat cropping. Geoderma 156 (3–4), 267–277.

Wiesenberg, G.L.B., Schwarzbauer, J., Schmidt, M.W.I., Schwark, L., 2004. Source and turnover of organic matter in agricultural soils derived from n-alkane/n-carboxylic acid compositions and C-isotope signatures. Org. Geochem. 35 (11–12), 1371–1393.

Wu, M.S., West, A.J., Feakins, S.J., 2019. Tropical soil profiles reveal the fate of plant wax biomarkers during soil storage. Org. Geochem. 128, 1–15.

Xiao, H., Li, Z., Chang, X., Huang, B., Nie, X., Liu, C., Liu, L., Wang, D., Jiang, J., 2018. The mineralization and sequestration of organic carbon in relation to agricultural soil erosion. Geoderma 329, 73–81.

Yang, S., Jansen, B., Absalah, S., Kalbitz, K., Cammeraat, E.L.H., 2020. Selective stabilization of soil fatty acids related to their carbon chain length and presence of double bonds in the Peruvian Andes. Geoderma 373, 114414.

Zhang, Y., Granger, S.G., Semenov, M.A., Upadhayay, H.R., Collins, A.L., 2022. Diffuse water pollution during recent extreme wet-weather in the UK: environmental damage costs and insight into the future? J. Clean. Prod. 338, 130633.